Available online at www.sciencedirect.com
ScienceDirect
Journal of the European Ceramic Society 29 (2009) 1721–1727
www.elsevier.com/locate/jeurceramsoc

Investigation of phase boundaries in the system $(K_xNa_{1-x})_{1-y}Li_y(Nb_{1-z}Ta_z)O_3$ using high-throughput experimentation (HTE)

Tobias A. Stegk, Henry Mgbemere, Ralf-Peter Herber, Rolf Janssen, Gerold A. Schneider *

Institute of Advanced Ceramics, Hamburg University of Technology, Denickestr. 15, 21073 Hamburg, Germany

Received 18 September 2008; received in revised form 16 October 2008; accepted 24 October 2008
Available online 12 December 2008

Abstract

A high-throughput experimental (HTE) approach starting from dry, fine-grained powders was used to synthesize bulk samples in the system $(K_xNa_{1-x})_{1-y}Li_y(Nb_{1-z}Ta_z)O_3$, a doped variant of the piezoelectric $(K_{0.5}Na_{0.5})NbO_3$ (KNN). Starting from the system $(K_{0.5}Na_{0.5})_{1-y}Li_y(Nb_{1-z}Ta_z)O_3$ known from the works of Saito et al. an effort was made to establish a higher order phase diagram. Special emphasis was put on expanding the known morphotropic phase boundary that constitutes a region of special interest for electroceramic materials as it features maximum piezoelectric properties. Analyses were performed using a HTE-compatible technique, namely automated powder X-ray diffraction (XRD).

Keywords: KNN; Powders-solid state reaction; Mixing; Niobates; Actuators; High-throughput experiemtation

1. Introduction

High-throughput experimentation (HTE) has been explained as "a set of techniques for creating a multiplicity of compounds and then testing them for activity".[1] It has been applied extensively for the development and optimization of ceramics mostly on the basis of thin-film technology since that allows for an easy continuous change of compositions and is therefore best suited for HTE.[1,2] For ceramic applications where macroscopic bulk properties are most important, e.g. in multilayer stack actuators, a different processing route is necessary. To emulate the most common powder metallurgical synthesis for ceramic materials, namely the conditioning, shaping and heat-treatment of powders, an HTE-setup has been conceived that has the capacity to produce libraries of up to 40 bulk samples at a time.[3] Drawing on the example of the yttria toughened zirconia polycrystal (Y-TZP) system, it was shown in Ref. 3 that it was possible to produce Y-TZP samples with a resolution of 0.5 mol.% and an experimental error of ~1 mol.% pertaining to yttria content. Synthesis and analysis were performed in high-throughput mode using dry ceramic powders as starting material.

In the present study, the dry powder HTE-setup was used to synthesize a variant of the system sodium potassium niobate ($K_{0.5}Na_{0.5}NbO_3$, KNN), a piezoelectric material that has the potential to substitute for lead zirconate titanate ($Pb(Ti_{1-x}Zr_x)O_3$, PZT) and hence to be used in the future in electronic appliances in the form of transducers or sensors.

PZT, a solid solution of $PbZrO_3$ and $PbTiO_3$, has been widely used in the manufacture of actuators, sensors, transducers and in other electromechanical devices because of its excellent piezoelectric properties. For commercial PZT-materials $x \approx 0.48$ which is coincident with a morphotropic phase boundary (MPB) between a rhombohedral and a tetragonal phase resulting in a maximum for the piezoelectric behaviour.[4] For actuator purposes the small signal d_{33} (piezoelectric coefficient) is used most often as a measure to compare the potential of different piezoceramics. As a benchmark for alternatives to PZT a d_{33} value of 300 pC/N is necessary. Additionally, the Curie temperature should be above 150 °C.

A substantial constituent of PZT however is formed by lead which is precarious since elemental lead is highly toxic. Due to its volatility it is released to the atmosphere during heat-

* Corresponding author. Tel.: +49 40 42878 3037; fax: +49 40 42878 2647.
E-mail address: g.schneider@tu-harburg.de (G.A. Schneider).

0955-2219/$ – see front matter © 2008 Elsevier Ltd. All rights reserved.
doi:10.1016/j.jeurceramsoc.2008.10.016

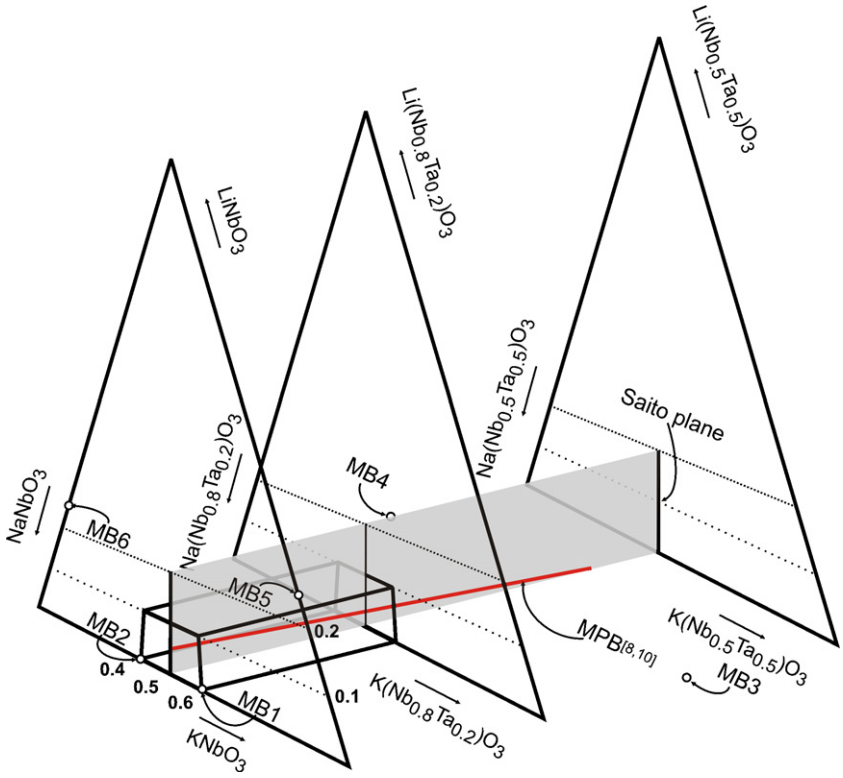

Fig. 1. Scheme of ternary phase diagram of $(K_xNa_{1-x})_{1-y}Li_y(Nb_{1-z}Ta_z)O_3$. The shaded area is the concentration plane examined in Refs. 8,10 here termed Saito-plane. The line located on the Saito-plane shows the approximate progression of the known morphotropic phase boundary. The dots labeled MB1-6 are the masterbatches used in the high-throughput synthesis of the library. The volume depicted between $RNbO_3$ and $R(Nb_{0.8}Ta_{0.2})O_3$ with R = K, Na, Li is the experimental space investigated in the present work.

treatment and furthermore it causes problems with respect to the disposal of PZT-based products at the end of their life cycle. The European Union has reacted on these environmental concerns by legal restrictions on the use of toxic lead.[5] These legal alterations have spawned interest in finding a lead-free replacement for PZT ceramics. Under amplified investigation is the perovskite family of KNN[6] for which three MPBs are reported in the literature so far, two in the system $K_xNa_{1-x}NbO_3$[7] and one in the system $(K_{0.5}Na_{0.5})_{1-y}Li_y(Nb_{1-z}Ta_z)O_3$.[8] Recently, the morphotropic nature of the phase boundary in the latter system separating an orthorhombic and tetragonal phase field could be verified experimentally[9] and d_{33} values between 200 and 300 pC/N have been reported along the MPB.[8,10] However, only for KNN prepared by a special texturisation procedure could maximum piezoelectric properties be achieved ($d_{33} > 300$ pC/N).[8] It is evident, that the textured synthesis of materials is complex and an implementation in cheap mass production is hence questionable. Furthermore, it is well known that KNN shows massive impediments in synthesis, namely difficulties when sintering and also the material's instability in air stemming from high reactivity with moisture has been reported.[11,12] Hence, the aspiration for replacement of PZT by a KNN-system necessitates efforts to overcome said impediments and to further optimize piezoelectric behaviour of conventionally synthesized KNN-materials.

Most of the investigations so far have been inside of or in close vicinity to the "Saito-plane", i.e. the concentration plane $(Na_{0.5}K_{0.5})_{1-y}Li_y(Nb_{1-z}Ta_z)O_3$ with $y \in [0,0.2]$ and $z \in [0,0.6]$ where the MPB was identified to behave approximately according to

$$y = 0.05 - 0.11z \quad (1)$$

It is obvious that the extension of this MPB line into a two-dimensional MPB area by opening the space in x-direction, i.e. changing the K/Na-ratio, offers new opportunities to find better piezoelectric compositions.

Consequently, this paper reports on the systematic expansion of the Saito-plane already investigated in Refs. 8,10 towards a concentration volume as depicted in Fig. 1. This concentration volume necessitates at least 100 different compositions for the respective phase space to be scanned sufficiently. As a consequence it is ideally suited for an HTE approach. Originating from the known location of the MPB line in the Saito-plane, the progression of the MPB into the mentioned concentration volume was determined on the basis of X-ray diffraction data.

2. Experimental

Initially six masterbatches for the HTE-procedure were synthesized using a conventional mixed carbonate and oxide route. Li_2CO_3, Na_2CO_3 and K_2CO_3 (99+% purity, ChemPur GmbH, Karlsruhe, Germany) as well as Nb_2O_5 and Ta_2O_5 (99.9% purity, ChemPur GmbH, Karlsruhe, Germany) were used as raw powders. All powders were dried at 200 °C

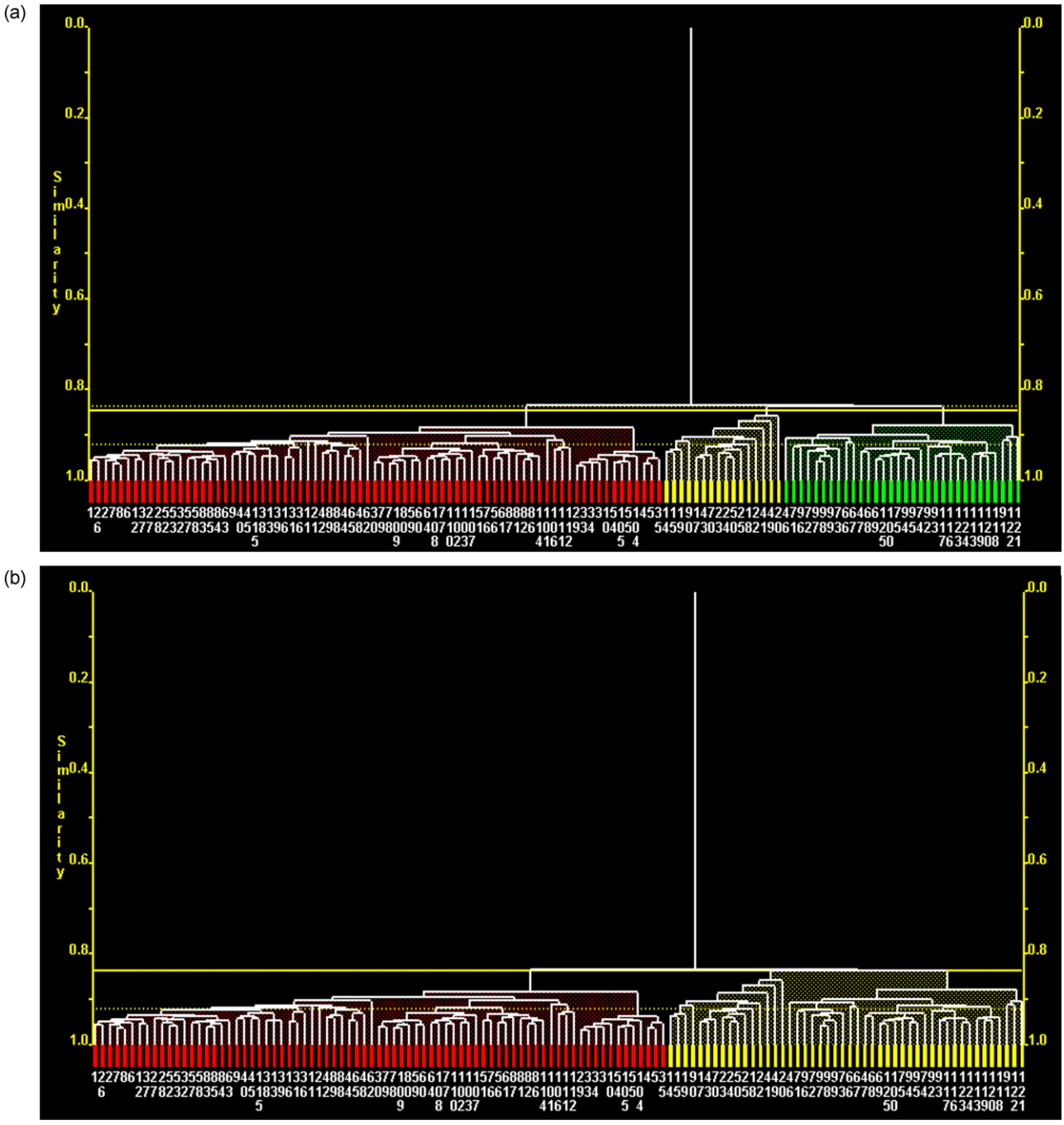

Fig. 2. Dendrograms as reported by PolySNAP: (a) manually restricted to three clusters and (b) manually restricted to two clusters.

for 5 h to remove all humidity and underwent pounding in a mortar before further processing. Subsequently, the powders were weighed in and attrition-milled for approximately 5 h. The milling was stopped when a predefined median ($d_{50} \approx 0.5\,\mu m$) of the grain size distribution was reached. The batches were 150 g each, and the milling took place in ethanol using 1000 g of grinding balls (diameter 3 mm, yttria-toughened zirconia, Tosoh, Tokyo, Japan). All batches were dried and homogenized after being milled. Three calcination cycles followed, conducted at 750 °C for 5 h. In between calcination the powders were repeatedly attrition-milled to expose new surface area and evoke a complete phase transformation. The resulting six masterbatches were $(K_{0.6}Na_{0.4})NbO_3$ (MB1), $(K_{0.4}Na_{0.6})NbO_3$ (MB2), $K(Nb_{0.65}Ta_{0.35})O_3$ (MB3), $Na(Nb_{0.65}Ta_{0.35})O_3$ (MB4), $(K_{0.75}Li_{0.25})NbO_3$ (MB5) and $(Na_{0.75}Li_{0.25})NbO_3$ (MB6).

Subsequently, using these masterbatches 125 samples of $(K_xNa_{1-x})_{1-y}Li_y(Nb_{1-z}Ta_z)O_3$ were synthesized with $x = [0.4, 0.45, 0.5, 0.55, 0.6]$, $y = [0,0.025, 0.05, 0.075, 0.1]$ and $z = [0,0.05, 0.1, 0.15, 0.2]$ according to the HTE-procedure highlighted in Ref. 3 The samples were processed in 5 groups of 25 samples, where each sample in one group shared the same

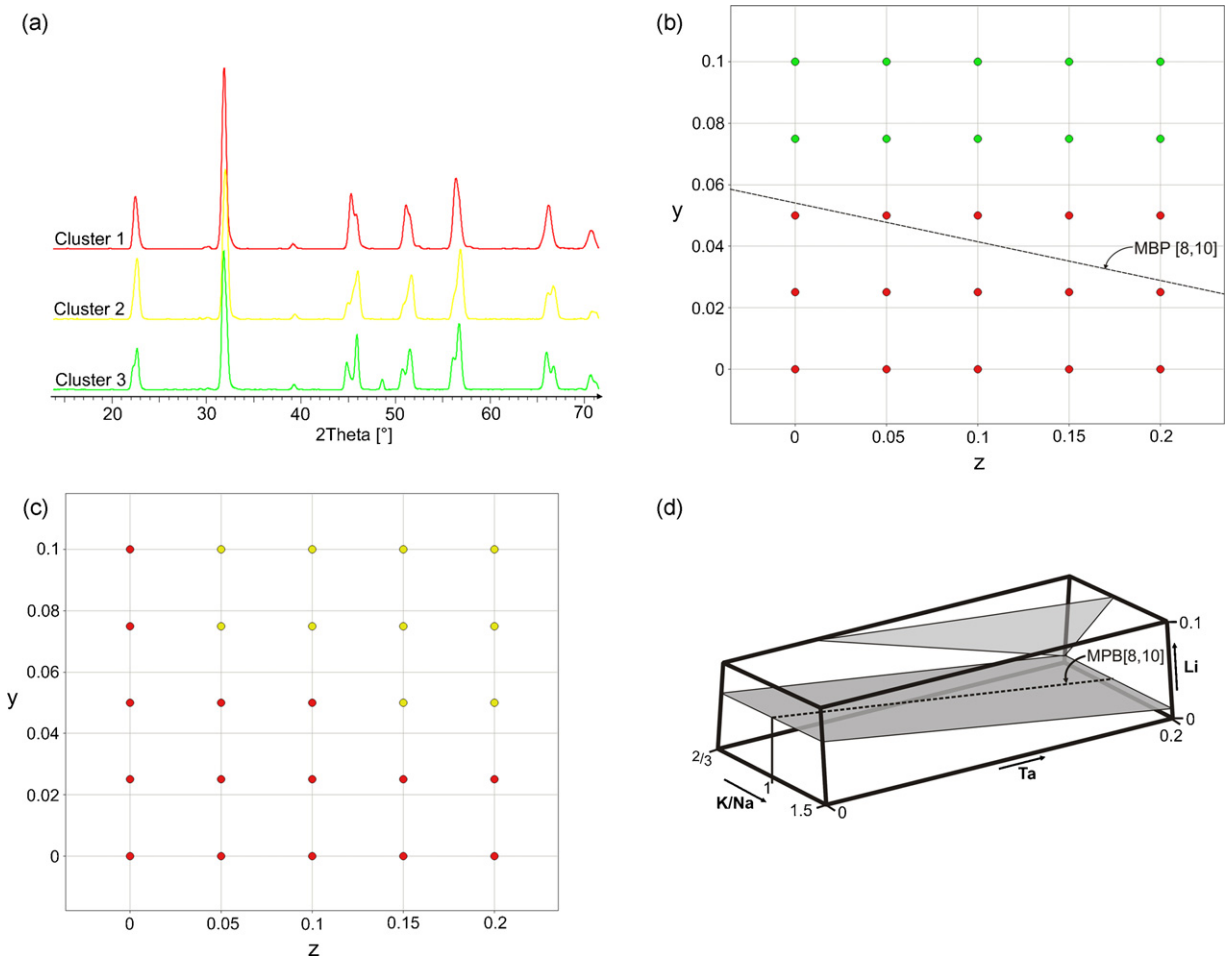

Fig. 3. Results of clustering as shown in Fig. 2a in color-coding (red: cluster 1, yellow: cluster 2, green: cluster 3). (a) XRD patterns of the most representative sample for each cluster. (b) Representation of Saito-plane ($x = 0.5$) with respective MPB (dashed line) superimposed and axes labels y and z being the other two stoichiometric coefficients in $(K_xNa_{1-x})_{1-y}Li_y(Nb_{1-z}Ta_z)O_3$. The colored dots mark the samples. The colors indicate the respective cluster affiliation with cluster 1 (red) identifying the orthorhombic and cluster 3 (green) the tetragonal phase according to Ref. 8. (c) Representation of concentration plane with $x = 0.4$. Note the presence of cluster 2 (yellow). (d) Scheme of the concentration volume examined. The two shaded areas represent the approximate progression of the cluster boundaries and hence hypothetical phase boundaries. The known linear section of the MPB is again depicted by the dashed line. (For interpretation of the references to color in this figure legend, the reader is referred to the web version of the article.)

x value with the x values themselves being randomized. y in turn, was completely randomized within x and z within y. This constituted three phased completely randomized block designs which in the literature is referred to as a split–split–plot[13] design and which has been suggested to be used for high-throughput experiments.[14] Note that the sample group with $x = 0.5$ in fact spanned a section of the Saito-plane and could hence be used for calibration purposes. Since some of the samples featured low melting phases, preliminary experimental cycles were needed to gradually lower the sintering temperature to a point where all samples were sintered but did not feature structural impediments due to excessive melting. All samples were sintered in air for 8 h at 990 °C. Samples were tablet-shaped and had a diameter of about 9 mm in the sintered state.

Analytic procedures were based on X-ray diffraction (XRD) on a D8 Discovery (Bruker AXS, Karlsruhe, Germany) equipped with Göbel mirror, general analysis diffraction detector system (GADDS). Using an automated xyz-table, a sequential treatment of up to 25 samples was possible at a time. Six independent XRD-patterns were recorded on various locations on the surface of any single sample between 15° and 70° 2θ. All the following analytic steps were performed on patterns that resulted out of an addition of those six single patterns. Thus one pattern per sample was created that held information averaged over the sample surface, hence limiting the effect of possible inhomogeneities.

The 125 patterns thus averaged were subsequently clustered. Clustering, also termed automatic classification, comprises a variety of methods to detect similarity in multivariate datasets and group those datasets accordingly.[15] The data are hence hierarchically nested according to a measure of distance or similarity and a customary way to report a clustering outcome is a tree-diagram or dendrogram with as many branches as there are objects in the dataset (125 in the case of this work).[16] The positions "down" the tree (along an axis of distance) at which two branches are linked (in mathematical graph theory referred to as nodes or vertices) are each marked by a specific distance or similarity value that states the limit for the two linked objects or subclusters to be in the same cluster. Algebraic procedures can be

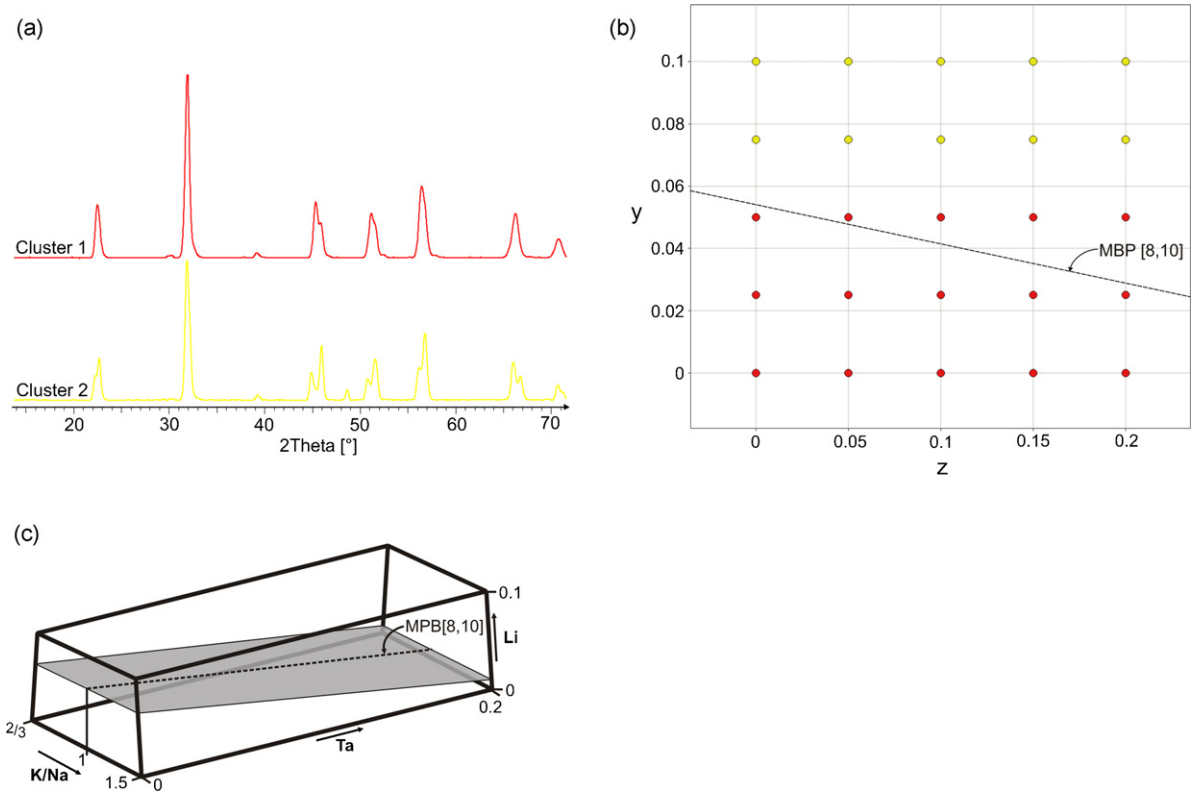

Fig. 4. Results of clustering as shown in Fig. 2b in color-coding (red: cluster 1, yellow: cluster 2). (a) XRD patterns of the most representative sample for each cluster. (b) Representation of Saito-plane ($x = 0.5$) with respective MPB (dashed line) superimposed and axes labels y and z being the other two stoichiometric coefficients in $(K_xNa_{1-x})_{1-y}Li_y(Nb_{1-z}Ta_z)O_3$. The colored dots mark the samples. The colors indicate the respective cluster affiliation with cluster 1 (red) identifying the orthorhombic and cluster 2 (yellow) the tetragonal phase according to Ref. 8. (c) Scheme of the concentration volume examined. The shaded area represents the approximate progression of the cluster boundary and hence hypothetical progression of the known morphotropic phase boundary, the known linear section of it again being depicted by the dashed line. (For interpretation of the references to color in this figure legend, the reader is referred to the web version of the article.)

used to determine how many clusters are present in one dataset. When using those, it is generally assumed that cutting a dendrogram at one specific height will create clusters of comparable homogeneity.[16]

The clustering in this work was performed using the commercial software PolySNAP that allowed the processing of datasets comprised of XRD-patterns.[17] It used a full pattern matching approach comparing each pair of patterns on a point-by-point basis and for the patterns in this study produced a 125×125 matrix holding a mean value of Pearson and Spearman correlation coefficients. Those correlation coefficients were transformed into normalized Euclidean distances or similarities with values between 0 (i.e. two patterns are completely unsimilar) and 1 (i.e. two patterns are the same). These similarity values were used as parameters for the clustering. Clustering was performed using the Group Average Link method, one of six methods included in PolySNAP. The result of the clustering was reported in the form of a dendrogram featuring, as a result of several eigenvalue operations, a cutoff distance that defined how many clusters were most likely to exist in the dataset. The cutoff line was flanked by confidence intervals derived from the highest and the lowest amount of clusters out of 15 estimates the program determined.[18] The interested reader is referred to Refs. 18,19 for more concise information on PolySNAP and especially its underlying mathematics.

The cut line could be moved manually and it was thus possible to increase or decrease the amount of clusters. This procedure was used such that in the Saito-plane the cluster boundary best mirrored the MPB known from Refs. 18,19 which could be achieved by either limiting the clusters to three (Fig. 2a) or two (Fig. 2b). It was assumed in these cases that the progression of the cluster boundaries through the investigated concentration volume would mirror the progression of the MPB and possible unknown phase boundaries.

3. Results and discussion

It is important to realize that the objective of HTE is to create a multitude of samples and subsequently test those for activity. The increase in throughput measured by the high amount of samples can be achieved by either parallel techniques or by automation of sequential techniques. One of the fundamentals of this approach is to choose the capacity of all the synthesis and analysis techniques in the same order of magnitude so as to avoid bottlenecks. Since at the time of writing XRD was the only analytic technique accessible to the authors that featured HTE-compatibility the results presented here are based solely on diffraction. Specifically, no microstructures or densities that would be part of the results of conventional materials science campaigns can be reported here.

In Fig. 2, clustering results from PolySNAP can be seen. Note the yellow bar being the cut line and the two dashed lines above and below marking the confidence intervals. For each cluster, PolySNAP also reported a most representative sample, i.e. the sample that had the minimum mean distance from all the other samples in the cluster.[19] The XRD-patterns of those are given in Figs. 3a and 4a. Furthermore, the progression of the MPB is shown against the outcome of the clustering procedure in Figs. 3b and 4b for the Saito-plane where clusters are color-coded. The clustering managed to reproduce the phase boundary reported in Refs. 8,10 reasonably well. It is obvious that in both clustering cases clusters were coherent inside the examined concentration space. This was the case not only for the Saito-plane illustrated here, but for the whole experimental space which suggested a gradual phase change within the clusters and hence physical credibility of the procedure.

In the case of three remaining clusters, it can be deduced that a third independent phase exists in the investigated sector. If this could be verified by more precise diffraction techniques at least one new phase boundary would ensue as depicted schematically in Fig. 3d. This could form an area of amplified examination due to the reasons mentioned above. Furthermore, the XRD-pattern belonging to cluster 2 in Fig. 3a showed features from both of the other patterns. This could also suggest a two-phase field with potential benefits analogous to the area around an MPB.

When two clusters were forced it was apparent that cluster 1 remained the same. This and the relatively good congruity between the known phase boundary and the cluster boundary hint to an MPB-area perpendicular to the area investigated by Saito et al. The benefits of the extension of the known MPB are twofold. It might be possible to find concentrations that surpass the piezoelectric behaviour reported by Saito et al. Secondly, compositions might arise that do not feature the synthesis difficulties known for KNN, namely the poor sinterability and high hygroscopicity.[12]

It has to be stated that the clustering fails to completely picture the MPB as is obvious from the deviation between MPB and cluster boundary in Figs. 3b and 4b. It was assumed that the reason for the deviation was the inaccuracy resulting out of the parallelized mixing procedure in our HTE-setup[3] and hence the MPB-area was adapted to the course of the phase boundary reported by Saito.

The mentioned inaccuracy has to be viewed against the savings of time due to the use of the HTE-setup. The 125 samples were synthesized, analysed and evaluated in 2 weeks. The evidence gained from this first experiment would have to be fed back into another experimental cycle, possibly zooming in on concentration regimes of interest, increasing the diligence of synthesis and the analytical effort.[20] Thus, this study has to be understood as a "First Stage Screen", as defined in Ref. 1.

4. Conclusion

A library of 125 samples in the system $(K_xNa_{1-x})_{1-y}Li_y(Nb_{1-z}Ta_z)O_3$ was synthesized and analysed using XRD. For this, an HTE-setup for dry powders was used allowing the full experimental cycle, excluding the preparation of the masterbatches, to be completed within two working weeks. The results with respect to phase development complement the work of Saito et al. by expanding the one-dimensional phase boundary line of their study into a two-dimensional MPB area. Furthermore, our results suggest the existence of a third phase or two phase field in the system holding potential benefits with respect to the exploitation of the material as a replacement for PZT. The relatively rough "First Stage Screen" reported here, will have to be followed up by more thorough investigations. These can be conducted more targeted through the structural information gained from this work.

Acknowledgement

The authors would like to acknowledge the valuable assistance of Mr. Michael Agthe in the preparation of sample libraries.

References

1. Cawse, J. N., Experimental strategies for combinatorial and high-throughput materials development. *Acc. Chem. Res.*, 2001, **34**, 213–221.
2. DECHEMA-Arbeitskreis Hochdurchsatzforschung für Materialien, Katalysatoren und Formulierungen. Positionspapier Hochdurchsatztechnologien in der Materialforschung. DECHEMA, Frankfurt a.M., 2006.
3. Stegk, T. A., Janssen, R. and Schneider, G. A., High-throughput synthesis and characterization of bulk ceramics from dry powders. *J. Combust. Chem.*, 2008, **10**, 274–279.
4. Moulson, A. J. and Herbert, J. M., *Electroceramics—Materials, Properties Applications*. Wiley, Chichester, 2003, pp. 354–358.
5. European Parliament and the Council. OJ L 37, 19, 2003.
6. Zhang, S., Xia, R. and Shrout, T. R., Lead-free piezoelectric ceramics vs. PZT? *J. Electroceram.*, 2007, **19**, 251–257.
7. Jaffe, B., Cook, W. and Jaffe, H., *Piezoelectric Ceramics*. Academic, New York, 1971, pp. 193–194.
8. Saito, Y., Hisaaki, T., Toshihiko, T., Nonoyama, T., Takatori, K., Homma, T. *et al.*, Lead-free piezocermics. *Nature*, 2004, **432**, 84–87.
9. Herber, R.-P., Schneider, G. A., Wagner, S. and Hoffmann, M. J., Characterization of ferroelectric domains in morphotropic potassium sodium niobate with scanning force microscopy. *Appl. Phys. Lett.*, 2007, **90**, 252905.
10. Saito, Y. and Takao, H., High performance lead-free piezoelectric ceramics in the (K, Na)NbO_3–$LiTaO_3$ solid solution system. *Ferroelectrics*, 2006, **338**, 17–32.
11. Kosec, K. and Kolar, D., On activated sintering and electrical properties of $NaKNbO_3$. *Mater. Res. Bull.*, 1975, **10**, 335–340.
12. Matsubara, M., Yamaguchi, T., Sakamoto, W., Kikuta, K., Yogo, T. and Hirano, S., Processing and piezoelectric properties of lead-free (K,Na)(Nb,Ta)O_3 ceramics. *J. Am. Ceram. Soc.*, 2005, **88**, 1190–1196.
13. Hinkelmann, K. and Kempthorne, O., *Design and Analysis of Experiments. Volume I. Introduction to Experimental Design*. Wiley, New York, 1994, pp. 453–454.
14. Cawse, J. N., *Experimental Design for Combinatorial and High Throughput Materials Development*. Wiley, Hoboken, 2003, pp. 129–145.
15. Johnson, M. A. and Maggiora, G. M., *Concepts and Applications of Molecular Similarity*. Wiley, New York, 1990, p. 47.

16. Gordon, A. D., *Classification: Methods for the Analysis of Multivariate Data*. Chapman and Hall, London, 1981, p. 33.
17. http://www.chem.gla.ac.uk/snap/PolySNAPindex.html.
18. Barr, G., Dong, W. and Gilmore, C. J., PolySNAP: a computer program for analysing high-throughput powder diffraction data. *J. Appl. Crystallogr.*, 2004, **37**, 658–664.
19. Barr, G., Dong, W. and Gilmore, C. J., High-throughput powder diffraction II. Applications of clustering methods and multivariate data analysis. *J. Appl. Crystallogr.*, 2004, **37**, 243–252.
20. Jandeleit, B., Schaefer, D. J., Powers, T. S., Turner, H. W. and Weinberg, W. H., Kombinatorische materialforschung und katalyse. *Angew. Chem.*, 1999, **111**, 2648–2689.